DOI: 10.1111/mice.12748

INDUSTRIAL APPLICATION

Sensitivity analysis and uncertainty quantification of a seismic risk model for road networks

Eduardo Allen[1] | Alondra Chamorro*[1,2] | Alan Poulos[1] | Sebastián Castro[1] | Juan Carlos de la Llera[1,3] | Tomás Echaveguren[1,4]

[1]Research Center for Integrated Disaster Risk Management (CIGIDEN), ANID/FONDAP/1511001, Chile
[2]Department of Construction Engineering and Management, School of Engineering, Pontificia Universidad Católica de Chile, Santiago, Chile
[3]Department of Structural and Geotechnical Engineering, School of Engineering, Pontificia Universidad Católica de Chile, Santiago, Chile
[4]Civil Engineering Department, Faculty of Engineering, Universidad de Concepción, Concepción, Chile

***Correspondence**
Alondra Chamorro. Email: achamorro@ing.puc.cl

Summary

Natural hazards may cause significant disruptions to road infrastructure, subsequently affecting road agencies, users, and productive activities. Despite the existence of infrastructure fragilities to seismic hazard and some operational consequences on network mobility, previous research has not modeled risk in terms of traffic disruptions and consequent travel time delays in subduction environments, analyzing the sensitivity to model parameters and quantified model uncertainty. This study proposes a risk framework to evaluate operational consequences in interurban road networks exposed to seismic hazard using travel time delays and propagate uncertainty in the model. Risk values are evaluated using Monte Carlo simulations and uncertainty is propagated using a polynomial chaos expansion meta-model. The framework was applied to a very critical interurban network in central Chile. Results demonstrate that the parameters that most significantly influence risk are fragility, loss of road capacity and traffic volume.

KEYWORDS:
Road network, Seismic risk analysis, Uncertainty quantification

1 | INTRODUCTION

Natural hazards may produce physical and subsequent operational effects on the road network, such as travel time delays, speed reductions or traffic congestion. According to Bil et al. (2014), these effects can be categorized as: (1) destruction of the infrastructure and permanent traffic interruption until the affected structures are restored; (2) partial structural damage that limits operation; and (3) traffic interruption without structural damage. The main purpose of transportation networks is to supply mobility, accessibility (AASHTO, 2011) and also to facilitate recovery after disruptive events (Duwadi & Pagán-Ortiz, 2013).

Network topology has been studied to assess the operational effects of natural events in terms of redundancy level and network complexity (e.g., Downer, 2009; Gao et al., 2019). Also, Javanbarg et al. (2008) highlighted the importance of redundancy from the perspective of optimal traffic assignment, its relation with operational impacts in unexpected events, and the optimal evaluation of mitigation strategies. Several indicators have been proposed to address this phenomenon in terms of travel capacity (Lee et al., 2011), connectivity (Bocchini & Frangopol, 2013), reliability of travel times (Zhang et al., 2015), flexibility of the capacity (Morlok & Chang, 2004), network coverage (S. E. Chang & Nojima, 2001), and redundancy indexes (Ip & Wang, 2011), among others. Nevertheless, most authors propose indicators to evaluate road network performance in urban environments (Tang & Huang, 2019) under normal operation conditions, i.e., not considering the physical damage produced by a natural event.

As an example of the relation between damaged road infrastructure and its operational consequences, the Northridge earthquake, California (1994) had an important impact on the

travel time due to damage to the Los Angeles road infrastructure. Indeed, two bridges of interstate highway I-10, connecting the city of Los Angeles and Santa Monica collapsed (Giuliano & Golob, 1998). Alternative routes were provided to mitigate the situation; however, the travel times increased significantly. For example, the average travel time for people living in north Los Angeles increased from 29.4 to 51.1 minutes to move from home to work, i.e., an increase of 73.8% (Giuliano & Golob, 1998).

Transportation networks exposed to natural hazards have been studied from different perspectives and with different objectives. For example, some studies have been focused in the definition and conceptualization of risk (e.g., Bil et al., 2014; Lowrance, 1976; Renn, 2008), the hazard modeling (Jayaram & Baker, 2010), the evaluation of performance indicators (e.g., Argyroudis et al., 2015; Faturechi & Miller-Hooks, 2015), direct losses (e.g., Kiremidjian, Moore, et al., 2007; Kiremidjian, Stergiou, & Lee, 2007) and resilience (Gao et al., 2019).

On the other hand, some studies have focused on the mitigation of the hazard effects in terms of infrastructure retrofit or evacuation processes. For example, in terms of infrastructure retrofit, L. Chang, Peng, et al. (2012) proposed a bridge retrofit program to maximize post-earthquake response in terms of highway capacity in Memphis, Fan et al. (2010) developed a two-stage stochastic program to optimize mitigation on bridges in Alameda County, and Huang et al. (2014) proposed an algorithm to minimize direct cost after seismic events through optimal bridge intervention. However, all these models are focuses on the optimization process after a particular hazard scenario in order to reduce the impact on bridges. In terms of evacuation processes, some works have focused on the implementation of algorithms for the design of road networks to mitigate the effects of natural hazards on evacuation routes after the events. For example, Nahum et al. (2017) developed a model for the design of an optimal evacuation network that minimizes cost and evacuation time under extreme conditions, Hadas & Laor (2013) proposed a new heuristic optimization model to design evacuation road networks in order to reduce travel times and Forcael et al. (2014) proposed a simulation model to define optimum evacuation routes during a tsunami using Ant Colony Algorithms (ACO), and demonstrated that the evacuation times obtained with their model are similar to the times observed in the field. Even though, these models have sophisticated optimization algorithms for evacuation design, they are focused on the reduction of cost and travel times after a potential event scenario and do not consider the potential effect of multiple scenarios or the probability of occurrence of them.

Interurban road networks are characterized by an uninterrupted associated flow but little topological redundancy, unlike urban road networks that have interrupted flows with high topological redundancy. This difference makes road infrastructure in interurban networks more critical since the collapse of certain infrastructure may lead to large travel time delays due to potential detours. In this respect, the transportation assignment model is essential to assess the consequences of road interruptions in terms of user travel times.

This study applies a simulation-based probabilistic seismic risk evaluation model that has been used in the literature for spatially distributed infrastructure (e.g., Argyroudis et al., 2015; Crowley & Bommer, 2006; Jayaram & Baker, 2010) and adapts it to evaluate operational consequences in road networks exposed to natural hazards using travel time delays. Furthermore, the study quantifies the epistemic uncertainty using a polynomial chaos expansion and the sensitivity of factors that affect the risk. The model considers different aspects, such as the hazard recurrence model, fragility of road assets, reduction in traffic capacity due to different damage states, flow assignment, evaluation of network performance, the evaluation of risk curves and the incidence of each factor to the total risk. The risk model and the uncertainty quantification model are applied in central Chile to evaluate the consequences on the road network due to the effect of the seismic hazard. Finally, the model has been developed for earthquake events but it can be adapted for other hazards.

2 | RISK MODELING OF ROAD NETWORKS EXPOSED TO SEISMIC HAZARD IN TERMS OF TRAVEL TIME

The risk assessment methodology considered in this study is based on the stochastic modeling of different consequences resulting from a set of synthetic realizations (scenarios). Risk assessment requires a wide understanding of the problem of interest, from the hazard to the system response. For instance, the transportation system can be affected by geological or hydro-meteorological hazards, which will affect in different ways the infrastructure and the traffic flow. Figure 1 presents the conceptual framework for assessing the risk of road networks. The model estimates risk in terms of the impact of multiple earthquakes on the road network and traffic after quake occurrence, once a transitory phase has ended. I.e., the model does not attempt to analyze the traffic process in a transient period immediately after the earthquakes.

The proposed framework (Figure 1) considers three steps: (1) input data; (2) processes; and (3) results. Input data corresponds to those originate by the models required for assessing risk. The hazard model is used to generate seismic scenarios with intensities at all locations. The road network assets model provides properties such as the location, lane numbers, lane capacity, free-flow speed and structural properties of bridges,

tunnels and roadways. The transportation model refers to the information regarding the origin-destination travels and flow.

The process begins with the characterization of the earthquake hazard through recurrence models calibrated in the study zone. After, the earthquake intensity (IM) in each highway asset location is estimated using a ground motion model (e.g., Abrahamson et al., 2016). Given the IM, damage states are sampled using fragility curves calibrated for each type of assets of the road network. A fragility curve specifies the probability of exceedance of different damage states given a certain intensity level (Mackie & Stojadinovic, 2004). This probability is represented by a probability distribution function (pdf) (e.g., Argyroudis et al., 2013; Basöz & Mander, 1999; G&E, 1994; Maruyama et al., 2010; NIBS, 2004), according to Equation 1.

$$F(im, \mu, \sigma) = \Phi\left(\frac{\ln(im) - \mu}{\sigma}\right) \quad (1)$$

In Equation 1, im is the hazard intensity; μ and σ are the parameters of the fragility function, which represent the mean and standard deviation of the natural logarithm intensity at which the damage state is reached respectively.$\Phi(\cdot)$ is the pdf of a standard normal distribution.

In order to sample the damage state for each realization and road asset, a random number seed is generated between 0 and 1 using a uniform distribution denoted as r_{nj} (a random number for the n-th realization and the j-th road asset). Table 1 shows the ranges of the random number used to assign one of four damage states to the road asset, based on the sampled r_{nj} value, where (μ_i, σ_i), $i = 1, 2$ and 3 are the parameters of the lognormal distribution associated with slight, moderate and severe damage state, respectively. Hence, each road asset adopts a single damage state in each realization.

Each damage state sets a highway capacity value. For instance, in the damage state "no damage", the highway capacity keeps constant and, for a "moderate" damage state, the highway capacity is lower than the one associated to "no damage" state. Once each asset damage state is obtained, the traffic

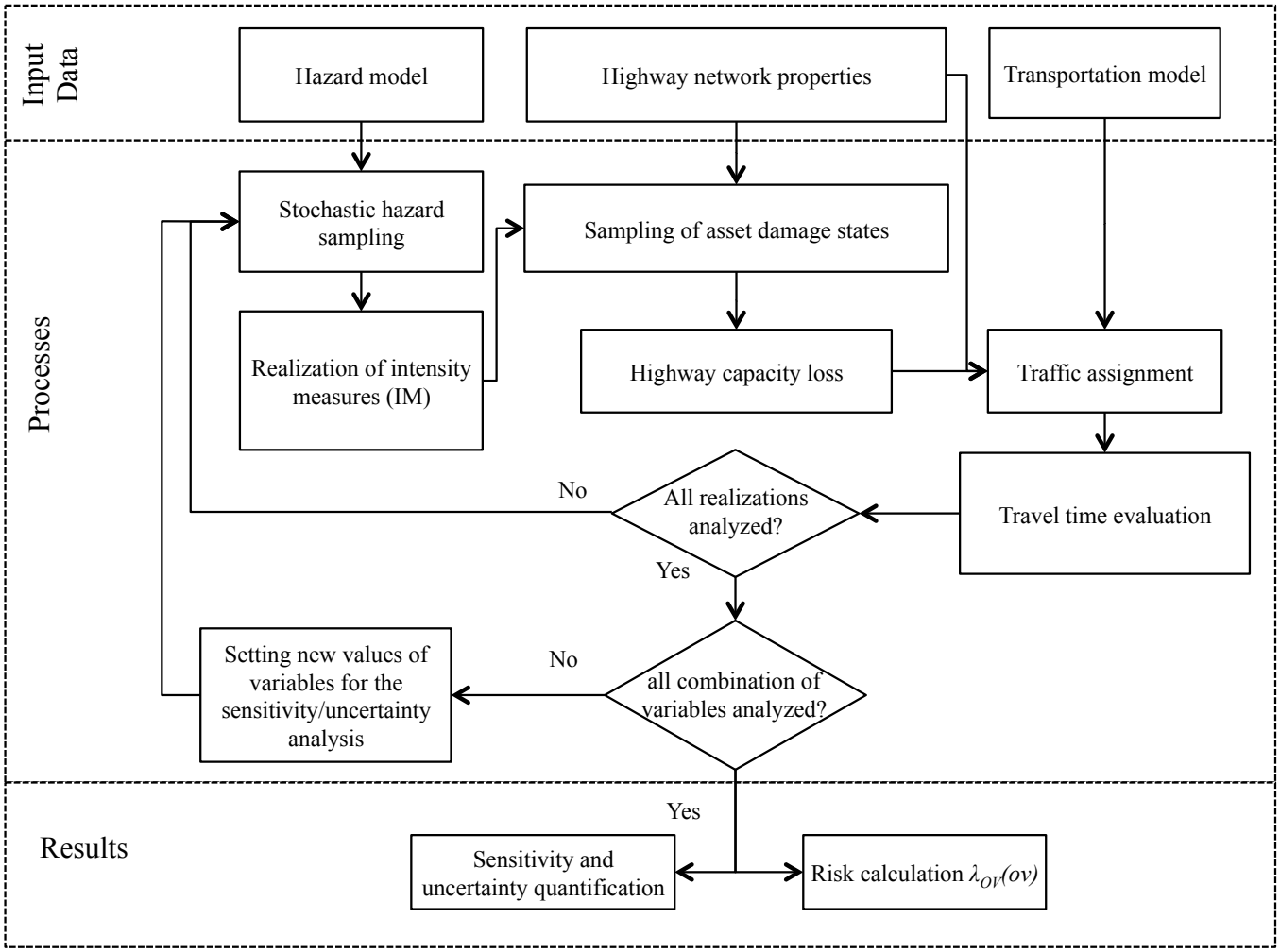

FIGURE 1 Conceptual framework of the road network risk evaluation

TABLE 1 Ranges used to assign damage states with a random number uniformly distributed between 0 and 1

Damage State	Condition
No damage	$r_{nj} \in \left[F(im, \mu_1, \sigma_1), 1\right]$
Slight damage	$r_{nj} \in \left[F(im, \mu_2, \sigma_2), F(im, \mu_1, \sigma_1)\right)$
Moderate damage	$r_{nj} \in \left[F(im, \mu_3, \sigma_3), F(im, \mu_2, \sigma_2)\right)$
Severe damage	$r_{nj} \in \left[0, F(im, \mu_3, \sigma_3)\right)$

is assigned to the highway network to obtain a new equilibrium, considering that after the earthquake there is a time lapse in which part of the road network is damaged with capacity and operating speed different to those before the earthquake. The configuration of origin-destination (OD) pairs and the travels between the OD pairs after an earthquake require special attention. As a consequence of a seismic event OD pairs may change, travels may decrease or the traffic daily patterns may change. These effects on the transportation system and traffic need to be studied on a case-by-case basis depending on the observed phenomena and available data. Furthermore, depending on the daily traffic variability, static or dynamic OD matrices may be required to reliably assign traffic to a network. If the traffic pattern in the road network is highly variable, the better option is to use the dynamic traffic assignment method (DTA). In contrast, if traffic is stable within the day, static traffic assignment (STA) may be suitable. The election of the proper traffic assignment approach depends on the daily traffic pattern and data availability

The transportation model considers the effect of different vehicle classes present on traffic flow, by using the passenger-car equivalent factors (pce) of Table 2 . The passenger-car equivalent is the number of passenger car displaced by a heavy vehicle under specified roadway, traffic and control conditions (HCM, 2016).

TABLE 2 Passenger Car Equivalent (pce) factors (HCM, 2016)

Type of vehicle	Equivalence factor (pdce)
Car (PC)	1
Bus (IUB)	1.5 - 2
Simple Truck (ST)	2 - 2.5
Double 2 Axles (DT)	2.5 - 3

The travel times are obtained using the user equilibrium principle first proposed by Beckmann et al. (1956), where each user aims to minimize his or her travel time. The link flows are obtained by solving the optimization problem presented in Equations (2)-(6).

$$\min \sum_{a \in A} \int_0^{f_a} t_a(u)\, \mathrm{d}u \tag{2}$$

subject to

$$\sum_{p \in P_W} h_p = T_W \,, \forall\, w \in W \tag{3}$$

$$f_a = \sum_{p \in P} \delta_{ap} \cdot h_p \,, \forall\, a \in A \tag{4}$$

$$h_p \geq 0 \,, \forall\, p \in P \tag{5}$$

$$f_a \geq 0 \,, \forall\, a \in A \tag{6}$$

In this model, w is an origin-destination pair; W is the set of all origin-destination pairs; P corresponds to all possible routes in the network; P_W is the subset of P with all the routes connecting the origin-destination pair w; p is a specific route in the network; T_W represents the demand in the origin-destination pair w; h_p is the flow in route p; f_a is the flow in link a; A is the set of all the links in the network; t_a is the travel time for link a; and δ_{ap} is Kronecker delta of whether link a belongs to route p (it takes the value 1 when link a belongs to the route, and the value 0 when it does not).

The constraint presented in Equation (3) establishes that travel demand for the origin-destination pair w must be equal to the sum of the flows of all routes connecting that origin-destination pair. The value of T_W comes directly from the origin-destination matrix, which reflects the user demand for traveling between different origin-destination pairs. Additionally, Equation (4) establishes that the flow of each link f_a must be equal to the sum of the flows of all routes passing through that link for all origin-destination pairs. Moreover, Equations (5) and (6) establish the conditions for positiveness of the flows.

The relation between travel time in each link and the assigned flow is obtained from the equations (7) and (8) for multi-lane highways and two-lane highways respectively HCM (2016).

$$t_a = t_a^o \left[1 + \alpha \left(\frac{f_a}{c_a}\right)^{\beta}\right] \tag{7}$$

$$t_a = \frac{d_a}{FFS_a - 0.0125 f_a - \epsilon_{np}} \tag{8}$$

where t_a is the travel time of link a; t_a^o is the travel time for link a under free-flow traffic conditions; f_a is the flow assigned to link a; c_a is the road capacity in terms of vehicles per hour; α and β are constants calibrated for each road category (HCM, 2016); FFS_a is the free-flow speed of link a; and ϵ_{np} is the adjustment factor to account no-passing zones on two-lane highways HCM (2016). Equation 8 is valid for different traffic ratios between lanes for two-lane roads. The effect

of asymmetric traffic per lane is considered by the factor f_{np}. Both equations are also valid for uncongested traffic. Therefore, delays on specific nodes in the network where the damage results in alternate traffic, delays can be emulated by setting low operating speed used in work zones areas.

These equations have been applied in extreme conditions resulting from natural event disruptions (e.g., Chamorro et al., 2020; L. Chang, Elnashai, & Spencer, 2012; Fan et al., 2010; Feng et al., 2020; Jayaram & Baker, 2010; Kiremidjian, Stergiou, & Lee, 2007). For example Feng et al. (2020) developed a scenario-based methodology to model the road network performance using the BPR function. Jayaram & Baker (2010) developed a new efficient hazard sampling model and applied it to the transportation system, where the travel time in each link is calculated based on the BPR function. Furthermore, Fan et al. (2010) optimized a mitigation program to reduce the impact of earthquakes in the road network and used BPR equations to estimate the relation between travel times and link flow.

To solve the traffic assignment through equations (3) – (7) there exist several algorithms, such us Frank-Wolfe's algorithm (Frank & Wolfe, 1956), the method of successive averages (MSA) (Sheffi & Powell, 1982) or the incremental assignment algorithm (ITA) (Martin & Manheum, 1965), among others. The election of the proper algorithms depends on the computation cost (which depends on the size of the road network), the number of realizations and the traffic patterns of the network.

The study aims to evaluate travel time between two nodes in inter-urban road networks once the transient phase of traffic assignment has ended and prior to the restoration process. Travel time is computed under the assumption that, given physical damage, highway capacity and average speed are reduced in the affected sections, and hence travel time increases. The origin-destination matrices do not change in this analysis.

Finally, risk is characterized by the mean annual frequency of an output variable OV, λ_{OV}, which represents the effect of the hazard scenario on the system, such as economic losses, infrastructure damage or travel time delay, among others (Mostafaei, 2013). The combinatoric nature of the problem and the complexity of evaluating all possible events of a given hazard make the problem amenable for an approximation through numerical simulations of the system's response. Therefore, a finite number of realizations of the hazard must be defined in order to perform a stochastic analysis of the system. To obtain the annual frequency of exceedance $\lambda_{OV}(ov)$, is necessary to evaluate the performance of the system for each realization and to record the exceedance (or not) of the output variable. The frequency of exceedance is estimated as the frequency of events multiplied by the proportion of events where a given value of the output variable, ov, is exceeded:

$$\lambda_{OV}(ov) = \nu E[I(ov_i > ov)] \approx \nu \frac{1}{n} \sum_{i=1}^{n} I(ov_i > ov) \quad (9)$$

where $E[\cdot]$ is the expected value; n is the number of simulations; ov_i is the value of the output variable for the i-th simulation; ν is the mean annual frequency of events; and $I(\cdot)$ is an indicator function, which is 1 if the argument is true and 0 if not. Depending on the variability of the hazard and the effect on the system, thousands of simulations could be required for this procedure to obtain results with an acceptable amount of error.

3 | RISK MODEL APPLICATION IN CENTRAL CHILE

The objective of this section is to apply the model to the interurban road network in central Chile and evaluate the eventual operational consequences, measured as changes in travel time, as a result of the disruption of seismic hazard.

The Chilean economy is highly dependent on port operation, which includes the transportation of imports and exports. In this context arises the interest of evaluating the effect of seismic events on the road network that connects the two main ports, San Antonio and Valparaiso, with Santiago, the main city of Chile. These two ports move more than 50% of the cargo, and new projects to increase their capacity are being analyzed (Ministry of Transport and Telecommunications of Chile, 2018).

The study evaluates travel time between two nodes in inter-urban road networks once the transient phase of traffic assignment has ended and prior to the restoration process. Travel time is computed under the assumption that, given physical damage, highway capacity and average speed are reduced in the affected sections, and hence travel time increases. The origin-destination matrices do not change in this analysis.

3.1 | Road network definition

The network considered corresponds to the inter-urban road network of the Metropolitana and Valparaiso regions, encompassing the main international, domestic, and regional routes, according to the categories described in the Chilean Highway Manual (MOP, 2019). The network under study has a length 2,072 km, from which 1,244 km are multi-lane roads and 828 km are two-lane highways (See Figure 2). The network has 59 bridges and 8 tunnels. The model of the road network of Figure 2 has 158 nodes and 173 links. The nodes represent the intersections and the links the roads, bridges and tunnels.

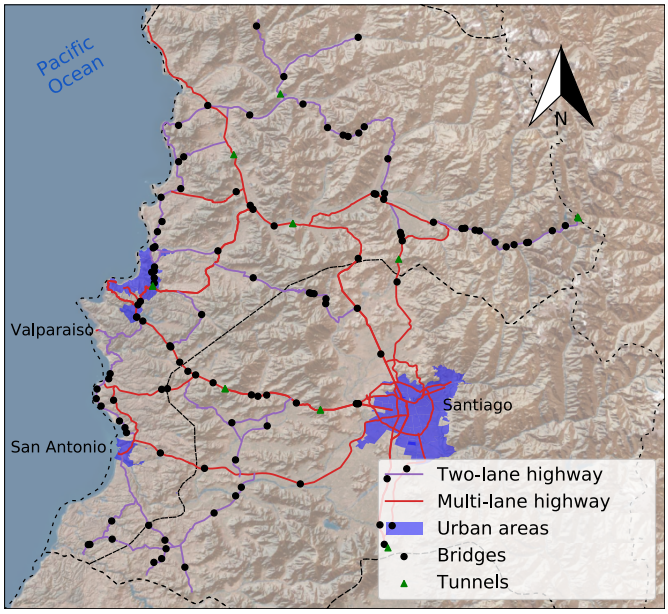

FIGURE 2 Road network of the central region of Chile

The multi-lane highways capacity was settled in 2400 pc/h/ln according to HCM (2016). The operating speed in two-lane highways was set at 70 km/h for the purposes of this modeling, which is modified according to the damage states.

The origin destination and traffic data was obtained from the National Traffic Survey of the Chilean Ministry of Public Works (MOP). The annual average daily traffic is 9,590 and 10,838 for the pairs Santiago - Valparaíso and Santiago - San Antonio respectively where the heavy vehicles represent the 13.7% and 12.7% respectively.

3.2 | Seismic hazard

The seismic risk of the network is assessed by evaluating its performance when subjected to a set of synthetic earthquake scenarios. The approach uses Monte Carlo simulations to generate these scenarios in order to consider different sources of uncertainty (Jayaram & Baker, 2010). The first step of the assessment consists in sampling earthquake sources, each with a magnitude and a hypocentral location. A total of 50,000 sources were sampled and their epicenters are shown in Figure 3 together with the components of the network. Only scenarios with epicenters that were closer than 500 km to at least one component of the system were considered. These sources are consistent with the local seismic hazard since they are generated by using a recently developed earthquake recurrence model developed for the study region (Poulos et al., 2019). This model separated the subduction seismicity of Chile into seven zones with distinct seismic productivity, geometry, and maximum magnitude. Western coastal zones generate subduction intraplate earthquakes along the boundary of the subducting Nazca Plate and the overriding South American Plate, whereas eastern zones generate subduction intraslab slab earthquakes within the Nazca Plate. The boundary between these two zones is highlighted by the differences in seismic productivity observed in Figure 3 . Shallow intraplate seismicity within the South American plate was not considered in this analysis due to its lower recurrence compared to subduction seismicity, its faster attenuation, and the reduced number of crustal faults near the network components.

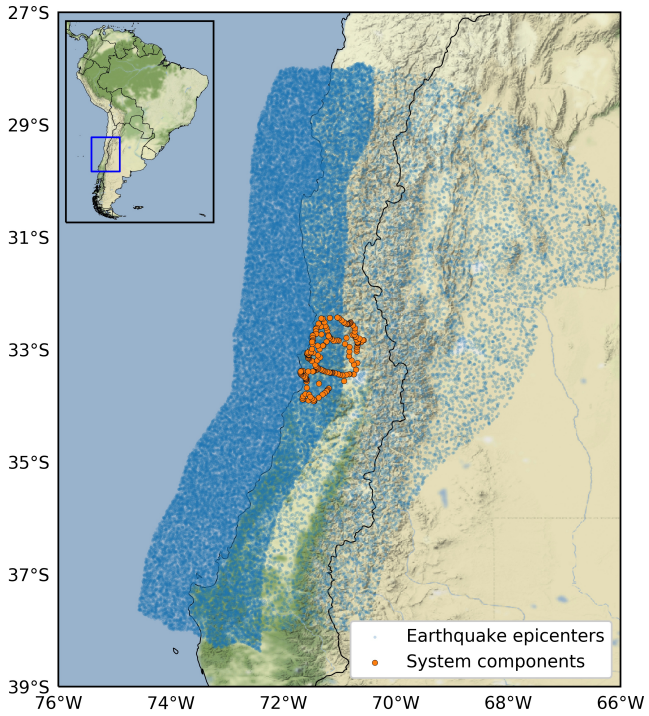

FIGURE 3 Locations of the epicenters of sampled seismic scenarios

In order to increase the computational efficiency, an importance sampling procedure proposed by (Poulos et al., 2017) was used, which samples earthquake magnitudes with a uniform distribution instead of their natural truncated exponential distribution. This sampling scheme increases the number of earthquakes with moderate to high magnitude, which has a greater contribution to the overall risk of the system than low magnitude earthquakes.

Once earthquake sources are sampled, the peak ground accelerations (PGA) at the locations of each system component are sampled using the following equation:

$$\ln(\mathrm{PGA}_{ij}) = \ln(\overline{\mathrm{PGA}}_{ij}) + \sigma_{ij}\varepsilon_{ij} + \tau_j\eta_j \qquad (10)$$

where PGA_{ij} is the sampled PGA that affects component i during earthquake j; $\overline{PGA}_{ij}$) is the median PGA affecting component i during earthquake j, which is computed using a ground motion model (GMM); σ_{ij} and τ_j are the intra-event and inter-event standard deviation terms, which are also obtained from a GMM; η_j is the normalized inter-event residual, sampled once for each earthquake scenario using a standard normal distribution; and ε_{ij} is the normalized intra-event residual, which is sampled from a multivariate normal distribution with zero mean, unit standard deviation, and a correlation structure derived elsewhere (Jayaram & Baker, 2009). The GMM used in this study was developed for subduction earthquakes using a global database (Abrahamson et al., 2016). Local soil conditions at the sites of the system components are considered in the GMM by using the average shear-wave velocity in the top 30 meters of soil, which were derived from a global database of the United States Geological Survey.

3.3 | Fragility of road assets

Fragility models developed by different authors were used in this study. Table 3 summarizes the lognormal parameters employed for each fragility curve and type of infrastructure, which are used in Equation (1) and Table 1 to sample damage states. The models adopted in this study consider Permanent Ground Displacement (PGD) as their intensity measure.

The expected permanent ground displacement due to liquefaction is calculated based on the methodology proposed by Joyner & Boore (1988), which is based on the soil liquefaction susceptibility indicator presented by Youd & Perkins (1987) and the ground motion attenuation relationship developed by Sadigh et al. (1986), which calculates the expected PGD for a specific site. To calculate the liquefaction susceptibility, the Chilean geological map (SERNAGEOMIN, 2003) is used and is related to susceptibility categories described by Youd & Perkins (1987).

TABLE 3 Parameters of log-normal fragility curves

Type of Assets	Slight		Moderate		Severe	
	μ	σ	μ	σ	μ	σ
Bridges (Basöz & Mander, 1999)	3.9	0.2	3.9	0.2	13.8	0.2
Tunnels (G&E, 1994)	6	0.7	12	0.7	60	0.5
Multi-lane (NIBS, 2004)	12	0.7	24	0.7	60	0.7
Two-lane (NIBS, 2004)	6	0.7	12	0.7	24	0.7

To evaluate the effect of physical damage on the road infrastructure, it is necessary to relate the damage states to a reduction in traffic capacity or speed. For Multi-lane highways, there is a reduction in traffic capacity. The factors are adapted from the values proposed by Shiraki et al. (2007) and Cartes (2017), which are 25% of reduction for slight damage, 50% for moderate damage and 100% of traffic capacity reduction for severe damage. On the other hand, for two-lane highways, the model considers a speed reduction of 55% for slight and moderate damage according to the values empirically observed by Hua et al. (2019) in work zones on these types of highways. The model considers a 100% speed reduction for severe damage. As described, the model considers the same speed reduction for slight and moderate damage based on the assumption that if a road has slight damage, the affected lane requires a temporary closing to remove debris. Hence, there is a need for a temporary work zone as well as the moderate damage.

3.4 | Travel time due to seismic hazard

The incremental assignment algorithm (ITA), first proposed by Martin & Manheum (1965), has been used in this study for its simplicity, convergence on simple networks, as the case study, and reduced computational time. This algorithm involves loading a portion of the O-D flows in each iteration and travel times updates for each link. For each iteration, the algorithm finds the shortest path between a specific pair of nodes and assigns the flow respectively. Then, the travel times for the links are updated according to equations (7) and (8). Results obtained with the ITA and the MSA were compared for three seismic scenarios, considering convergence, computational effort and resulting travel times of the models. MSA was carried out using the algorithm proposed by Kumar (2019). Results present differences lower than 10% in terms of travel times for both routes. Computational times per seismic scenario, however, were 500 seconds for MSA and less than 2 seconds for ITA to converge. For the 50,000 seismic scenarios and 5,000 risk cases considered in the sensitivity analysis MSA takes considerably more time than ITA, reason why the latter was considered for the risk and sensitivity analyses.

For the evaluation of multi-lane roads, equation 7 is used according to HCM (2016). For two-lane roads, equation 8 is used, which includes a factor that depends on the flow distribution in both directions and no-passing zones. However, the use of cost functions that integrates the flow of both directions to model asymmetries has been omitted (we only consider the factor of equation 8) due to the lack of calibrated models for the study area.

The evaluation of the network performance is based on the simulation of 50,000 seismic realizations. The code was developed on Python and all simulations were performed on Ubuntu

Server 16.04 with Intel(R) Xeon(R) CPU E5-2660 processors. The simulations, i.e. the 50,000 scenarios, took 48.5 seconds using 50 cores. Figure 4 shows the results of the network performance, measured as travel times between the cities of Santiago and Valparaiso for the different simulations.

Figure 4 a shows the distribution of the Expected Travel Times obtained from the simulations with respect to the earthquake magnitude. It is clear that for magnitudes lower than 7.0 Mw there is almost no travel delay. For higher magnitudes, however, an exponential distribution was adjusted in order to estimate the effect of the magnitude in the expected travel time. For each one of the three magnitude ranges presented in Figure 4 b, the CDF was calculated, which allows us to quantify the effect of the earthquake magnitude in the network. From this analysis, the mean travel time for the three magnitude ranges, from lowest to the highest, are 1.42 hrs, 3.98 hrs and 6.9 hrs respectively. However, while this analysis is helpful in understanding the earthquake effect on the system given a certain magnitude range, this does not consider the hazard recurrence. It is necessary to highlight that the results obtained in Figure 4 represent systemic consequences for the simulated set of earthquakes, i.e. earthquakes with epicenters closer than 500 km to at least one component of the network. Changing the region where epicenters are sampled would alter the distributions of Figure 4 . On the other hand, a travel time comparative analysis was made between Santiago - San Antonio and Santiago - Valparaiso. Figure 5 shows a comparative analysis between the mean annual frequencies of exceedance for expected travel times between these two urban areas.

The curves conceptually show that network redundancy, in terms of alternative routes, is a determining factor when assessing risk, a fact that is reflected in the shape of the curves. The route between Santiago and San Antonio has only two totally independent roads (without common links). On the other hand, the route connecting Santiago and Valparaiso has three completely independent routes and several other routes that allow reassigning the flow to reach the destination. Consequently, the high expected travel times between Santiago and Valparaiso are reached with seismic events that are much less frequent than those required for Santiago-San Antonio. For example, expected travel times of 5 hours are reached with a mean annual frequency of $3.56 \cdot 10^{-3}$ for Santiago-Valparaiso and $5.54 \cdot 10^{-3}$ for Santiago-San Antonio, which correspond to return periods of 280 and 180 years, respectively.

The impacts of increases in travel time can be quantified in terms of the cost of time of each vehicle in the network. For

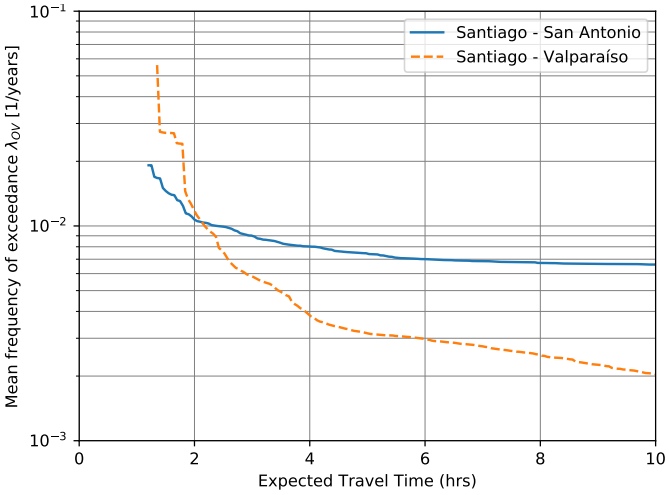

FIGURE 5 Mean annual frequencies of exceeding different levels of average travel times for the Santiago - San Antonio and Santiago - Valparaiso urban areas.

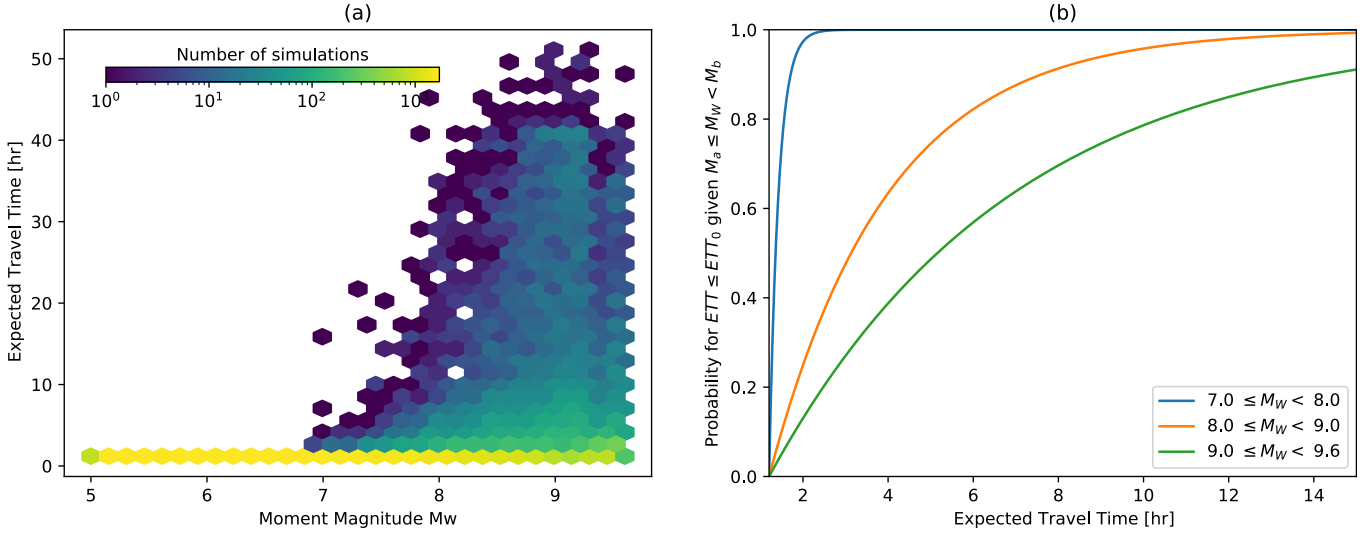

FIGURE 4 Road network performance for simulated seismic realizations for Santiago - Valparaiso

each seismic scenario, the total cost of the network was calculated according to the costs of time proposed by MDS (2021), which correspond to 20.45 USD for passenger cars, 12.47 USD for trucks and 235.5 USD for inter-urban buses. Figure 6 shows the mean frequency of exceedance of over-costs for the road network travel time delays for one day.

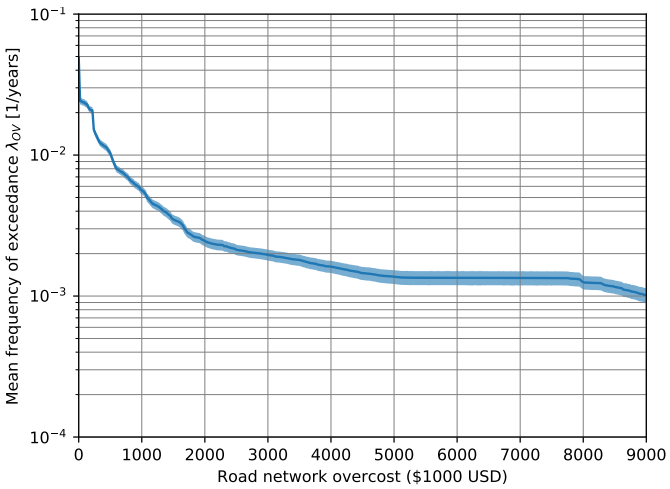

FIGURE 6 Mean annual frequencies of exceeding different road network over-costs due to travel time delays.

The applied traffic assignment model does not consider the effect of the variation of the origin-destination matrix as a result of a natural event and assumes that these values are static over time. Therefore, the obtained results do not represent the traffic phenomenon immediately after the event, but they do represent the operational effects on the interurban road network once the origin-destination matrix has been reestablished, but the road infrastructure has not been recovered. A more detailed study of the variations of post-event origin-destination matrices is required to seize the systemic effect immediately after the natural event. A further approach of the transportation model is related to the origin-destination matrices considering the Annual Average Daily Traffic (AADT); consequently, this application does not reflect the time and seasonal effects of each one of the events. One way to incorporate these uncertainties is through a stochastic simulation that samples time-dependent origin-destination matrices.

3.5 | Topological analysis of the network

To better analyze the effect of topology in terms of redundancy in the network and the effect in travel time delays, the model was applied to two cases: (1) the redundant network (see Figure 2); and (2) direct routes only. Figure 7 shows the routes considered as the direct from Santiago to San Antonio and Valparaiso.

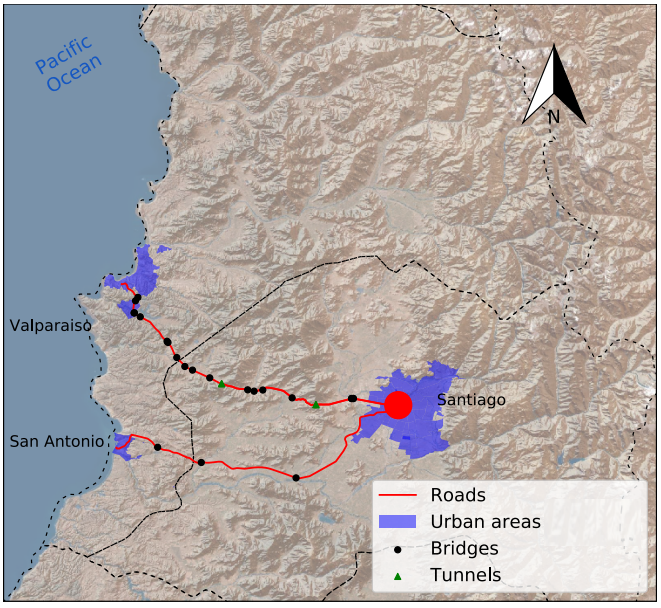

FIGURE 7 Road network without redundancy

Figure 8 summarizes the results of the redundancy analysis, representing the mean annual frequency of exceedance curves for the connections (a) Santiago - San Antonio and (b) Santiago - Valparaiso. The results show that the connectivity between Santiago and San Antonio has low redundancy and that the seismic hazard effects are quite similar if one considers only the direct route instead of all routes.

On the other hand, Figure 8 b shows the redundancy effect for Santiago – Valparaiso. In this case, the curve without redundancy reaches an asymptote because the travel time between both cities tends to infinity without decreasing the frequency of the seismic event. This occurs when an asset of the direct route presents severe damage (total traffic interruption), and since there are no alternative routes, there can be no traffic reassignment. If alternative routes are present, there is traffic reassignment, and the frequency of events continues to decrease while increasing expected travel times.

The obtained results demonstrate that redundancy in both networks plays a key role when evaluating the travel time delays as a result of each seismic scenario. The travel times for both routes (Santiago-San Antonio and Santiago-Valparaiso), under free-flow traffic conditions, are similar. However, when considering seismic scenarios, the network connecting Santiago and San Antonio presented greater susceptibility to travel time delays, due to the fact that it has few alternative routes and the flow distribution induced a high cost (in terms of travel time) for the links connecting both locations. These results

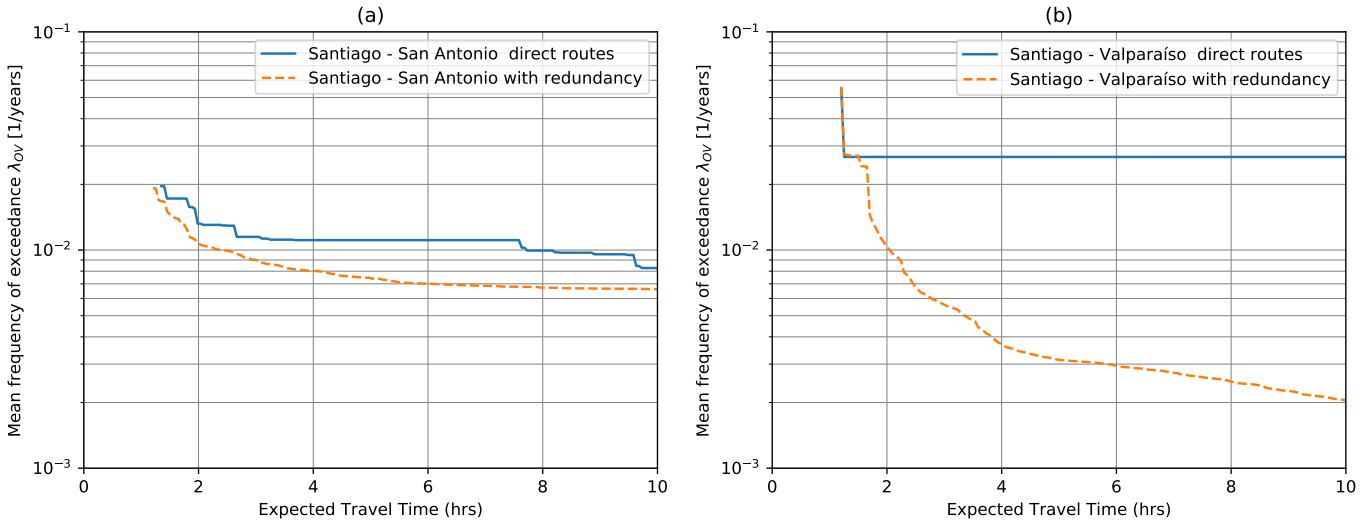

FIGURE 8 Redundancy effect on the road network

suggest that the risk of a road network exposed to a natural hazard is highly dependent on the interaction among the elements, represented by the existence of redundant roads; if there is a flow distribution possibility, the effect on travel times is reduced.

4 | SENSITIVITY ANALYSIS AND UNCERTAINTY QUANTIFICATION

Once the risk has been computed for the road network with the respective redundancy analysis, it is necessary to evaluate the incidence of each of the parameters described above on the total risk. On the other hand, the propagation of uncertainty behind the models is quantified. This section evaluates the incidence of the parameters and quantifies the uncertainty of the model described above for the road network. However, this model can be applied to quantify uncertainty in any type of network.

4.1 | Polynomial Chaos Expansion method

Polynomial chaos expansion (PCE) models have gained great popularity in recent years due to their efficiency in global sensitivity analysis with multivariate output (Garcia-Cabrejo & Valocchi, 2014). These models have been applied to recent engineering problems (e.g., Hariri-Ardebili & Sudret, 2020; Hurtado et al., 2017; Ni et al., 2019). This meta-model consists of approximating the output of a system by using a polynomial expansion that combines the input parameters using a polynomial basis of functions. A presentation of the method can be found in Sudret (2008). In essence, the expansion defines an input random vector $\boldsymbol{X} = \{X_1, X_2, \dots, X_M\}$ that represents M random input variables. The PCE method applied to the output $\lambda_{OV}(ov)$ may be expressed by

$$\lambda_{OV}(ov, \boldsymbol{X}) = \sum_{\alpha \in \mathbb{N}^M} y_\alpha(ov)\Psi_\alpha(\boldsymbol{X}) \tag{11}$$

where y_α are the coefficients of the polynomial function and Ψ_α are the basis functions. The sum considers an infinite series of polynomial functions, which is truncated in practice. Additionally, the use of a multivariate orthonormal polynomial basis with respect to the multivariate probability distribution of the input variables, $f_{\boldsymbol{X}}(\boldsymbol{x})$, implies that

$$y_\alpha(ov) = \int_\Omega \lambda_{OV}(ov, \boldsymbol{x})\Psi_\alpha(\boldsymbol{x})f_{\boldsymbol{X}}(\boldsymbol{x})\, \mathrm{d}\boldsymbol{x} \tag{12}$$

where Ω is the space of all input parameters. Notice that the calculation of the coefficients $y_\alpha(ov)$ requires the evaluation of λ_{OV}, which is the function that needs to be approximated.

For the truncated PCE model used herein, six random variables were considered: the median values (μ) of the fragility curves for each type of structure (bridge, tunnel, single and multi-lanes), the road capacity for moderate damage, and the volume traffic ratio. These parameters are considered independent, and their distributions and polynomial basis are presented in Table 4 .

The coefficients for each mean rate of exceedance of the expected travel time were obtained using the UQLab library (Marelli & Sudret, 2014) by sampling 5,000 points (each evaluation requires the same 50,000 seismic scenarios) and using a least-angle regression methodology to estimate a sparse truncated PCE (Blatman & Sudret, 2011). The maximum order of the truncated PCE is set at 14. This computation took around 3 days for the evaluation of the 5,000 points, and 1.5 days for the PCE coefficients calculation considering 1,000

TABLE 4 Meta-model input parameters

Variable	Description	Distribution	Polynomial basis
α_1	Multiplier factor of the median value for bridge fragility curves	$U(0.5, 1.5)$	Legendre
α_2	Multiplier factor of the median value for single lane fragility curves	$U(0.5, 1.5)$	Legendre
α_3	Multiplier factor of the median value for tunnel fragility curves	$U(0.5, 1.5)$	Legendre
α_4	Multiplier factor of the median value for multi lane fragility curves	$U(0.5, 1.5)$	Legendre
D_{mod}	Capacity reduction factor for moderate damage state	$U(0.25, 0.75)$	Legendre
V	Traffic volume ratio with respect to the mean annual volume	$N(1, 0.08^2)$	Hermite

points for each mean frequency of exceedance curve. The precision of the PCE model was evaluated using the leave-one-out (LOO) cross-validation error and is presented in Figure 9 . The largest estimated error is less than 5.3%, which is considered acceptable.

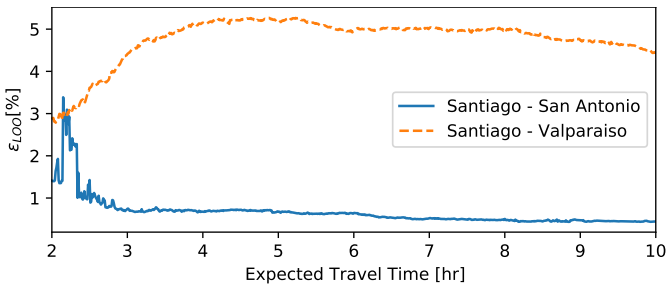

FIGURE 9 LOO cross validation of the truncated sparse PCE model for both cases.

4.2 | Sensitivity analysis and uncertainty quantification

The truncated sparse PCE model obtained is used in two different analyses. First, a sensitivity analysis to estimate the impact of each input parameter in the variability of the output. And secondly to quantify the uncertainty of the output due to the random nature of the input parameters.

For the sensitivity analysis, the Sobol method was used, which quantifies the ratio of the variance of each input parameter to the variance of the final result (Sobol, 1993). The Sobol index for an input parameter X_i is defined by

$$S_i = \frac{\mathrm{Var}(\mathrm{E}[\lambda_{OV}|X_i])}{\mathrm{Var}(\lambda_{OV})} \tag{13}$$

which represents the ratio between the variance of the expected value of output given a value of X_i and the total variance of the model. This analysis is done for all input parameters and the interactions between them (second and higher order Sobol indices). Additionally, Sudret (2008) showed that the Sobol indices of a truncated PCE model can be established analytically.

Figure 10 shows the evolution of the first order Sobol indices for the expected travel time in both cases, Santiago - San Antonio and Santiago - Valparaiso. In both cases, the parameter that has the most impact on the results is α_4, which relates to the fragilities of multi-lane highways. This was expected since the direct routes between Santiago and the two ports are multi-lane, and any failure of these two routes implies detours and travel time delays. The fragility curve parameters associated with other types of assets have a negligible contribution to the overall variance. The main difference in both routes is the contribution of D_{mod} and V along with the expected travel time. For the pair Santiago - Valparaiso, the parameter V is more relevant than D_{mod} and that could be explained by the redundancy effect shown in Figure 8 . Indeed, Santiago -

Valparaiso has more redundancy, and hence the D_{mod} parameter has a lower contribution than it does for the pair Santiago - San Antonio. In the latter, there are more independent routes between the two cities and the traffic could be reassigned in case of capacity loss.

The relevance of one factor over others reflects the behavior of the particular network. For example, as presented in Figure 10 , traffic volume is more relevant on the Santiago - Valparaíso route, being more dependent to hourly and monthly variations. To better address the potential effects of hourly variations, the application of a dynamic traffic analysis would be adequate if accurate data is available. To emulate the effect of a peak hour and an off-peak hour scenarios, the demand was modified by +/- 50% and then the risk curves were modeled. The variation of the mean annual frequancy of exceedance as a result of traffic changes is approximately 15% more in the case of Santiago - Valparaíso. The three different scenarios show the relevance of the traffic level in the Santiago – Valparaíso route in accordance to the sensitivity analysis.

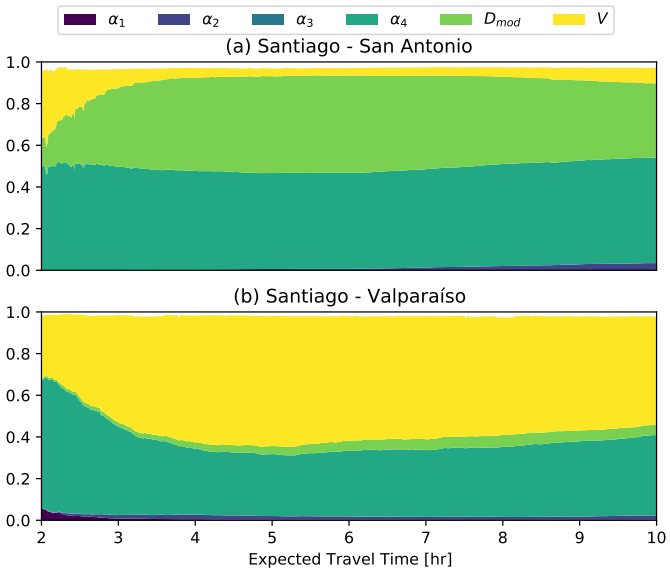

FIGURE 10 Graphical representation of the first order Sobol indices for routes (a) Santiago - San Antonio, and (b) Santiago - Valparaiso. Each color represents the contribution of the corresponding parameter to the total variance of the output. The white area corresponds to higher order Sobol indices contribution.

Furthermore, uncertainty quantification was performed by evaluating the truncated sparse PCE model with 20,000 samples of the input parameters. The obtained distributions for the risk curves given the uncertainties of the input parameters are presented in Figure 11 for both Santiago - San Antonio and Santiago - Valparaiso cases. The coefficient of variation for the San Antonio route decreases from 25.5% to 22.8%, but increases from around 17.5% to 31% in the case of Valparaiso. This is seen by percentile intervals that are almost constant in the San Antonio case while they increase in the Valparaiso case. This difference is explained by the variation in the relevance of each parameter along the travel time presented in Figure 10 , where the impact on travel times of the fragility curves for multi-lane highways and the capacity loss, are almost constant. In the case of Valparaiso, the most influential parameters are the fragilities for multi-lane highways, capacity loss factor and the traffic volume, which are strongly related to the expected travel time, thus generating uncertainty in the total risk.

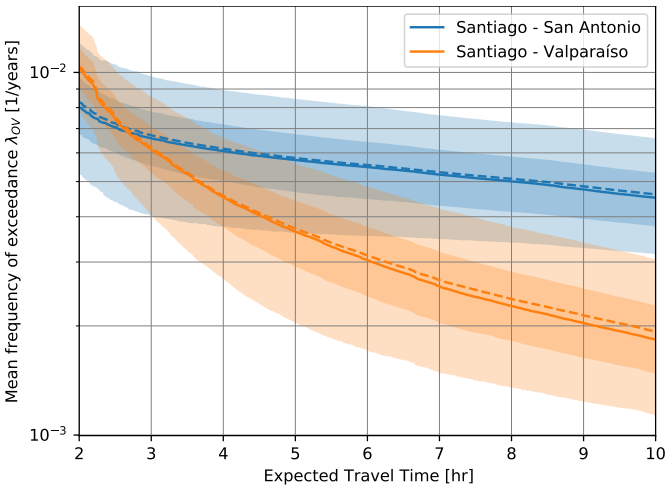

FIGURE 11 Risk curves for the expected travel time for Santiago - San Antonio and Santiago - Valparaiso. Solid lines are the median values, dashed lines the mean values, darker areas the 25-75 percentile intervals and lighter areas the 5-95 percentile intervals.

5 | CONCLUSIONS

This research presents a probabilistic approach to estimate the earthquake risk of a road network. The model estimates the operational consequences of this single natural hazard in terms of travel times. The model was applied to the seismic risk of a road network in central Chile, obtaining expected travel time between the capital Santiago and the two largest ports in the country, Valparaiso and San Antonio.

The expected travel time between these nodes is controlled by the redundancy of the network. The connection Santiago – Valparaiso has more independent paths, and more redundancy than the connection Santiago – San Antonio. As shown

in Section 3.5, the latter connection presents greater susceptibility to increase travel time due to seismic events. Therefore, redundancy plays a key role in reducing the risk in travel times for this road network.

A sensitivity analysis was carried out to assess the impact of six parameters on the estimated seismic risk. The most relevant parameter is the fragility of multi-lane highways. These results may have direct policy implications. For example in the Santiago - San Antonio connection, where fragility and capacity have greater relevance, is indicative of the need to strengthen infrastructure and network redundancy, while for the connection Santiago - Valparaiso, where the traffic volume parameter is relevant, policies should focus on controlling traffic levels since there is more redundancy, which decreases the negative consequences produced by the physical failure. However, as the sensitivity analysis showed, both routes are highly dependent on multi-lane highway fragility, which is basically explained because the main routes that connect Santiago and the ports are multi-lane highways.

The study can be used to evaluate the effectiveness of different mitigation strategies applied to road infrastructure and the effects in travel time, as well as the identification of critical links, need for redundancy and the analysis of capacity improvements. The model can also be used to estimate mitigation and restoration costs, as well as user costs resulting from increased travel time. Furthermore, the model can also be used for the risk assessment of new road projects in the network. As demonstrated in the study, redundancy is essential to decrease the impact of earthquakes. Therefore, the risk analysis presented in this study could support the feasibility of a new project in order to reduce the impact of natural hazards.

This study also revealed the need to expand research in different areas. One of them is the estimation of the origin-destination matrices immediately after a natural event since the present study assumed that trips did not change as a consequence of the earthquake and, hence, it was not able to capture the change in demand, which could modify the operational consequences on the network. Results showed that traffic volume is a key factor in the evaluation of travel time delays. The research could also be expanded in terms of traffic modeling with other assignment algorithms that may integrate asymmetries in two-lane roads and in terms of hourly variations during peak hours through a dynamic traffic assignment (DTA). The use of dynamic analysis is critical when there are variations in flow throughout the day. For example, in urban areas that present peak. Another source of future research is the application of the model in urban environments and the integration of a congestion model.

Travel time delays between the locations defined in each seismic scenario have different causes. One of the main factors is the quality of fragility functions used in the study and the intensity measures considered. This study adopted the functions proposed by different authors in the literature; however, these functions were calibrated to meet local conditions and may not necessarily represent the fragility of each asset considered in this study. On the other hand, different intensity measures may be associated with different failure mechanisms. This research uses only permanent ground deformation and neglects failures of road infrastructure caused by ground and spectral accelerations. These models were taken due to the lack of fragility functions for road assets specifically calibrated for Chile.

Finally, this model was developed for seismic hazard. However, it could be used with hazards such as volcanic or hydrometeorological events. Extensions to other hazards require infrastructure fragility curves, hazard recurrence models and attenuation models to estimate the hazard intensity fields.

ACKNOWLEDGEMENTS

The authors thank the National Research and Development Agency (ANID), which has financed the FONDEF Project ID14I20309 Research and Development of Models to Quantify and Mitigate the Risk of Natural Hazards in the National Road Network, FONDECYT Project ID181754 Socio-economic modeling of mitigation strategies for resilient critical infrastructure: Application to drink water systems and road networks, FONDECYT Project ID1170836 SIBER-RISK: SImulation Based Earthquake Risk and Resilience of Interdependent Systems and Networks. Likewise, we express our gratitude to the institutions that participated and contributed to this research project, especially to the Research Center for Integrated Disaster Risk Management ANID/FONDAP/15110017 (CIGIDEN) and the Highways Department of the Chilean Ministry of Public Works.

References

AASHTO. (2011). *Transportation asset management guide: A focus on implementation*. Washington, DC: American Association of State Highway and Transportation Officials.

Abrahamson, N., Gregor, N., & Addo, K. (2016). Bc hydro ground motion prediction equations for subduction earthquakes. *Earthquake Spectra*, *32*(1), 23–44.

Argyroudis, S., Kaynia, A., & Pitilakis, K. (2013). Development of fragility functions for geotechnical constructions: Application to cantilever retaining walls. *Soil Dynamics and Earthquake Engineering*, *50*, 106–116.

Argyroudis, S., Selva, J., Gehl, P., & Pitilakis, K. (2015). Systemic seismic risk assessment of road networks

considering interactions with the built environment. *Computer-Aided Civil and Infrastructure Engineering*, *30*(7), 524-540.

Basöz, N., & Mander, J. (1999). *Enhancement of the highway transportation lifeline module in HAZUS* (Tech. Rep.). Washington, D.C.: National Institute of Building Sciences.

Beckmann, M., McGuire, C., & Winsten, C. (1956). *Studies in the economics of transportation*. New Haven, CT: Yale University Press.

Bil, M., Sedonik, J., Kubecek, J., Vodak, R., & Bolova, M. (2014). Road network segments at risk - vulnerability analysis and natural hazards assessment. *The Science for Population Protection*, *6*. Retrieved from http://www.population-protection.eu/prilohy/casopis/eng/20/87.pdf.

Blatman, G., & Sudret, B. (2011). Adaptive sparse polynomial chaos expansion based on least angle regression. *Journal of Computational Physics*, *230*(6), 2345–2367.

Bocchini, P., & Frangopol, D. M. (2013). Connectivity-based optimal scheduling for maintenance of bridge networks. *Journal of Engineering Mechanics*, *139*(6), 760–769.

Cartes, P. (2017). *Modelo de selección de medidas de mitigación asociadas a eventos naturales en carreteras* (Bachelor's Thesis). Universidad de Concepción, Chile.

Chamorro, A., Echaveguren, T., Allen, E., Contreras, M., Dagá, J., de Solminihac, H., & Lara, L. E. (2020). Sustainable risk management of rural road networks exposed to natural hazards: Application to volcanic lahars in chile. *Sustainability*, *12*(17), 6774.

Chang, L., Elnashai, A., & Spencer, B. (2012). Post-earthquake modelling of transportation networks. *Structure and Infrastructure Engineering*, *8*, 893-911.

Chang, L., Peng, F., Ouyang, Y., Elnashai, A., & Spencer, B. (2012). Bridge seismic retrofit program planning to maximize postearthquake transportation network capacity. *Journal of Infrastructure Systems*, *18*, 75-88.

Chang, S. E., & Nojima, N. (2001). Measuring post-disaster transportation system performance: the 1995 kobe earthquake in comparative perspective. *Transportation Research Part A: Policy and Practice*, *35*(6), 475–494.

Crowley, H., & Bommer, J. J. (2006). Modelling seismic hazard in earthquake loss models with spatially distributed exposure. *Bulletin of Earthquake Engineering*, *4*(3), 249–273.

Downer, J. (2009). *When failure is an option: Redundancy, reliability and regulation in complex technical systems*. London, U.K.: Centre for Analysis of Risk and Regulation, London School of Economics and Political Science.

Duwadi, S. R., & Pagán-Ortiz, J. E. (2013). Reducción de riesgo a desastres por medio de carreteras resilientes: Un programa de investigación y desarrollo. *Rev. Int. de Desastres Naturales, Accidentes e Infraestructura Civil*, *13*(1).

Fan, Y., Liu, C., Lee, R., & Kiremidjian, A. S. (2010). Highway network retrofit under seismic hazard. *Journal of Infrastructure Systems*, *16*(3), 181–187.

Faturechi, R., & Miller-Hooks, E. (2015). Measuring the performance of transportation infrastructure systems in disasters: A comprehensive review. *Journal of Infrastructure Systems*, *21*, 04014025.

Feng, K., Li, Q., & Ellingwood, B. R. (2020). Post-earthquake modelling of transportation networks using an agent-based model. *Structure and Infrastructure Engineering*, *16*(11), 1578-1592.

Forcael, E., González, V., Orozco, F., Vargas, S., Pantoja, A., & Moscoso, P. (2014). Ant colony optimization model for tsunamis evacuation routes. *Computer-Aided Civil and Infrastructure Engineering*, *29*(10), 723-737.

Frank, M., & Wolfe, P. (1956). An algorithm for quadratic programming. *Naval Research Logistics Quarterly*, *3*(1-2), 95-110.

Gao, L., Liu, X., Liu, Y., Wang, P., Deng, M., Zhu, Q., & Li, H. (2019). Measuring road network topology vulnerability by ricci curvature. *Physica A: Statistical Mechanics and its Applications*, *527*, 121071.

Garcia-Cabrejo, O., & Valocchi, A. (2014). Global sensitivity analysis for multivariate output using polynomial chaos expansion. *Reliability Engineering & System Safety*, *126*, 25–36.

G&E. (1994). *NIBS earthquake estimation methods technical manual* (Tech. Rep.). G&E Engineering System.

Giuliano, G., & Golob, J. (1998). Impacts of the northridge earthquake on transit and highway use. *Journal of Transportation and Statistics*, *1*(2), 1–20.

Hadas, Y., & Laor, A. (2013). Network design model with evacuation constraints. *Transportation Research Part A: Policy and Practice*, *47*, 1-9.

Hariri-Ardebili, M. A., & Sudret, B. (2020). Polynomial chaos expansion for uncertainty quantification of dam engineering problems. *Engineering Structures*, *203*, 109631.

HCM. (2016). *Highway capacity manual* (6th ed.). Washington, D.C.: Transportation Research Board.

Hua, X., Wang, Y., Yu, W., Zhu, W., & Wang, W. (2019). Control strategy optimization for two-lane highway lane-closure work zones. *Sustainability*, *11*, 4567.

Huang, Y., Parmelee, S., & Pang, W. (2014). Optimal retrofit scheme for highway network under seismic hazards. *International Journal of Transportation Science and Technology*, *3*(2), 109 - 128.

Hurtado, D. E., Castro, S., & Madrid, P. (2017). Uncertainty quantification of 2 models of cardiac electromechanics. *International Journal for Numerical Methods in Biomedical Engineering*, *33*(12), e2894.

Ip, W. H., & Wang, D. (2011). Resilience and friability of transportation networks: evaluation, analysis and optimization. *IEEE Systems Journal*, *5*(2), 189–198.

Javanbarg, M., Takada, S., & Kuwata, Y. (2008). Priority evaluation of seismic mitigation in pipeline networks using multicriteria analysis fuzzy ahp. In *14th world conference on earthquake engineering.* Beijing, China.

Jayaram, N., & Baker, J. W. (2009). Correlation model for spatially distributed ground-motion intensities. *Earthquake Engineering & Structural Dynamics*, *38*(15), 1687–1708.

Jayaram, N., & Baker, J. W. (2010). Efficient sampling and data reduction techniques for probabilistic seismic lifeline risk assessment. *Earthquake Engineering & Structural Dynamics*, *39*(10), 1109–1131.

Joyner, W. B., & Boore, D. M. (1988). Measurement, characterization, and prediction of strong ground motion. In *Earthquake engineering and soil dynamics ii, proceedings of american society of civil engineers geotechnical engineering division specialty conference* (pp. 43–102). Park City, Utah.

Kiremidjian, A. S., Moore, J., Fan, Y. Y., Yazlali, O., Basoz, N., & Williams, M. (2007). Seismic risk assessment of transportation network systems. *Journal of Earthquake Engineering*, *11*(3), 371-382.

Kiremidjian, A. S., Stergiou, E., & Lee, R. (2007). Issues in seismic risk assessment of transportation networks. In K. D. Pitilakis (Ed.), *Earthquake geotechnical engineering* (Vol. 6, pp. 461–480). Dordrecht: Springer.

Kumar, P. (2019). *prameshk/Traffic-Assignment: Static Traffic Assignment using User Equilibrium and Stochastic User Equilibrium- Python Code.* Zenodo. Retrieved from https://doi.org/10.5281/zenodo.3479554

Lee, Y.-J., Song, J., Gardoni, P., & Lim, H.-W. (2011). Post-hazard flow capacity of bridge transportation network considering structural deterioration of bridges. *Structure and Infrastructure Engineering*, *7*(7-8), 509–521.

Lowrance, W. W. (1976). *Of acceptable risk: Science and the determination of safety*. Los Altos, CA: William Kaufmann Inc.

Mackie, K., & Stojadinovic, B. (2004). Fragility curves for reinforced concrete highway overpass bridges. In *13th world conference on earthquake engineering.* Vancouver BC, Canada.

Marelli, S., & Sudret, B. (2014). UQLab: A framework for uncertainty quantification in MATLAB. In *The 2nd international conference on vulnerability and risk analysis and management (ICVRAM 2014)* (p. 2554-2563). University of Liverpool, UK.

Martin, B., & Manheum, M. (1965). A research program for comparison of traffic assignment techniques. *Highway Research Record*.

Maruyama, Y., Yamazaki, F., Mizuno, K., Tsuchiya, Y., & Yogai, H. (2010). Fragility curves for expressway embankments based on damage datasets after recent earthquakes in japan. *Soil Dynamics and Earthquake Engineering*, *30*, 1158-1167.

MDS. (2021). *Precios sociales* (Tech. Rep.). Santiago: Ministerio de Desarrollo Social y Familia.

Ministry of Transport and Telecommunications of Chile. (2018). *Gobierno realizará histórica inversion portuaria en region de valparaíso para potencial la capacidad logística del país con miras al 2030.* Retrieved from https://www.mtt.gob.cl/archivos/17806.

MOP. (2019). *Manual de carreteras* (Tech. Rep.). Chile: Dirección de vialidad, Ministerio de Obras Públicas. Retrieved from https://mc.mop.gob.cl.

Morlok, E. K., & Chang, D. J. (2004). Measuring capacity flexibility of a transportation system. *Transportation Research Part A: Policy and Practice*, *38*(6), 405–420.

Mostafaei, H. (2013). Vulnerability assessment of reinforced concrete structures for fire and earthquake risk. In S. Tesfamariam & K. Goda (Eds.), *Handbook of seismic risk analysis and management of civil infrastructure systems* (pp. 366–386). Woodhead Publishing.

Nahum, O. E., Hadas, Y., Rossi, R., Gastaldi, M., & Gecchele, G. (2017). Network design model with evacuation constraints under uncertainty. *Transportation Research Procedia*, *22*, 489 - 498.

Ni, P., Xia, Y., Li, J., & Hao, H. (2019). Using polynomial chaos expansion for uncertainty and sensitivity analysis of bridge structures. *Mechanical Systems and Signal Processing*, *119*, 293–311.

NIBS. (2004). *HAZUS-MH: user's manual and technical manuals* (Tech. Rep.). Washington, DC: National Institute of Building Sciences.

Poulos, A., Espinoza, S., de la Llera, J., & Rudnick, H. (2017). Seismic risk assessment of spatially distributed electric power systems. In *16th world conference on earthquake engineering.* Santiago, Chile.

Poulos, A., Monsalve, M., Zamora, N., & de la Llera, J. C. (2019). An updated recurrence model for chilean subduction seismicity and statistical validation of its poisson nature. *Bulletin of the Seismological Society of America*, *109*(1), 66–74.

Renn, O. (2008). White paper on risk governance: Toward an integrative framework. In O. Renn & K. D. Walker (Eds.), *Global risk governance: Concept and practice using the IRGC framework* (Vol. 1, pp. 3–73). Dordrecht: Springer.

Sadigh, K., Egan, J., & Youngs, R. (1986). Specification of ground motion for seismic design of long period structures. *Earthquake Notes*, *57*(1), 13.

SERNAGEOMIN. (2003). *Mapa geológico de chile (pdf file)*. Retrieved from https://www.u-cursos.cl/usuario/74db06406c5f883b052c2d22911d03db/mi_blog/r/MAPA.pdf.

Sheffi, Y., & Powell, W. B. (1982). An algorithm for the equilibrium assignment problem with random link times. *Networks*, *12*(2), 191-207.

Shiraki, N., Shinozuka, M., Moore, J. E., Chang, S. E., Kameda, H., & Tanaka, S. (2007). System risk curves: probabilistic performance scenarios for highway networks subject to earthquake damage. *Journal of Infrastructure Systems*, *13*(1), 43–54.

Sobol, I. M. (1993). Sensitivity estimates for nonlinear mathematical models. *Mathematical modelling and computational experiments*, *1*(4), 407–414.

Sudret, B. (2008). Global sensitivity analysis using polynomial chaos expansions. *Reliability Engineering & System Safety*, *93*(7), 964–979.

Tang, Y., & Huang, S. (2019). Assessing seismic vulnerability of urban road networks by a bayesian network approach. *Transportation Research Part D: Transport and Environment*, *77*, 390 - 402.

Youd, T. L., & Perkins, D. M. (1987). Mapping of liquefaction severity index. *Journal of Geotechnical Engineering*, *113*(11), 1374–1392.

Zhang, W., Cao, M., & Wang, N. (2015). Travel time reliability based bridge network maintenance optimization under budget constraint. In *12th international conference on applications of statistics and probability in civil engineering, ICASP12*. Vancouver, Canada.

How to cite this article: Allen E, Chamorro A, Poulos A, Castro S, de la Llera JC, Echaveguren T, Sensitivity analysis and uncertainty quantification of a seismic risk model for road networks. *Comput Aided Civ Inf*, 2022;37:516–530. https://doi.org/10.1111/mice.12748